

# Fast and optimal nonparametric sequential design for astronomical observations

JUSTIN J. YANG

*Department of Statistics,  
Harvard University*

juchenjustinyang@fas.harvard.edu

XUFEI WANG

*Department of Statistics,  
Harvard University*

xufeiwang@fas.harvard.edu

PAVLOS PROTOPAPAS

*Institute for Applied Computational Science,  
Harvard School of Engineering and Applied Sciences*

pavlos@seas.harvard.edu

LUKE BORNN

*Department of Statistics,  
Harvard University*

bornn@stat.harvard.edu

March 1, 2024

## Abstract

The spectral energy distribution (SED) is a relatively easy way for astronomers to distinguish between different astronomical objects such as galaxies, black holes, and stellar objects. By comparing the observations from a source at different frequencies with template models, astronomers are able to infer the type of this observed object. In this paper, we take a Bayesian model averaging perspective to learn astronomical objects, employing a Bayesian nonparametric approach to accommodate the deviation from convex combinations of known log-SEDs. To effectively use telescope time for observations, we then study Bayesian nonparametric sequential experimental design without conjugacy, in which we use sequential Monte Carlo as an efficient tool to maximize the volume of information stored in the posterior distribution of the parameters of interest. A new technique for performing inferences in log-Gaussian Cox processes called the Poisson log-normal approximation is also proposed. Simulations show the speed, accuracy, and usefulness of our method. While the strategy we propose in this paper is brand new in the astronomy literature, the inferential techniques developed apply to more general nonparametric sequential experimental design problems.

**Keywords:** Bayesian nonparametric, sequential experimental design, sequential Monte Carlo, spectral energy distribution, Bayesian model averaging, log-Gaussian Cox processes, Poisson log-normal approximation

## 1 Introduction

Spectral energy distributions (SEDs), as well as their fitting, are used in many branches of astronomy to characterize astronomical sources. For example, photometric redshift estimation (distance estimation of sources) relies heavily on the SED morphology of galaxies. Because of its strong predictive power and relative ease of use, SED fitting is very commonly used in astronomy.

Our *scientific goal* in this paper is to fit telescope observations to various existing template SEDs, which are generated either from observations of known astronomical objects or models, in order to (i) classify a

new astronomical source, (ii) analyze a new blended source as a geometrically weighted average of template models, or (iii) detect the evidence of a new type of SED which cannot be directly described by known templates.

However, due to the high cost of using sophisticated telescopes and the limitation of observation time, it is necessary to carefully design the observational strategy using all the information we have, including the template models, the specifications of telescope filters<sup>1</sup>, and those existing observations. In the context of SED fitting, this is equivalent to specify the set of filters to use in order to better achieve the aforementioned scientific goal. Decisions regarding these specifications must be made before the data collection. Because specific information is usually available prior to the use of the telescope, the Bayesian framework will play an important role.

Especially, sequential design is preferred as opposed to a non-sequential one. The following three advantages motivate our choice of this methodology: Firstly, the optimal sequential design procedure must be at least as good as a fixed design procedure (Chaloner and Verdinelli [1995]). Secondly, it is usually more computationally efficient, as finding the optimal non-sequential design for all design variables at a time is usually NP-hard (Ko et al. [1995]). Finally, a sequential design can also incorporate the existing literatures on multi-armed bandit problems (Robbins [1952], Berry and Fristedt [1985], Krause and Ong [2011]) and sequential Monte Carlo (SMC) (Cherkassky and Bornn [2013]).

Our *statistical goal* in this paper is to provide an efficient and fast calculation scheme to reach the optimal sequential design under the SED fitting context. One computational difficulty comes from the incorporation of a *non-conjugate* Bayesian nonparametric prior on the deviation between the (convex combinations of) template models and the truth. It is this non-conjugate setting that makes our work different from the existing literatures in *Bayesian nonparametric sequential experimental design (BNS-ED)*, which usually assumes a Gaussian conjugacy.

There are several major contributions we make in this paper. We are the first to our knowledge to study BNS-ED without conjugacy. Our second contribution is to provide a fast SMC algorithm to solve the general BNS-ED problems. Furthermore, by employing the special model structure of log-Gaussian Cox process (LGCP), the main model of interest in this paper, we introduce a new technique called Poisson log-normal approximation (PoLNA) to improve computation speed. As a third contribution, we apply the new methodology stated above to sequentially choose the best filters to use and fit the SED on-the-fly. To show how our method could be applied, we perform simulation tests on real astronomical templates and demonstrate that, using our algorithm, one can better analyze the unknown SED in terms of template

---

<sup>1</sup>Filters here mean the physical filters used with the detectors on the telescope in order to restrict the observed electromagnetic bandwidth, a range of frequencies.

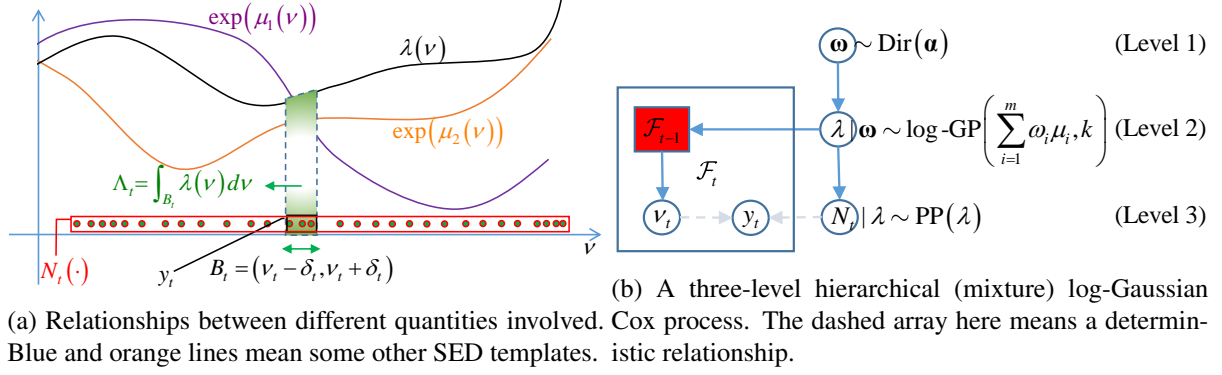


Figure 1: Graphical illustrations for the problem of SED fitting as well as its model setting.

models with fewer observations, which shows the practical value of our methodology.

The rest of this paper is organized as follows. In Section 2, we formulate the main scientific problem of interest and specify the quantities and notations we will use throughout this paper. In Section 3, we introduce the statistical model, design perspective, and general SMC inferential scheme for BNS-ED. We then introduce the specialized technique PoLNA for LGCP in Section 4. Simulation examples are provided in Section 5. Finally, we discuss several related works and conclude in Section 6. We leave more detailed calculations to the Supplementary Material.

## 2 Motivation

A graphical illustration for the problem of fitting a spectral energy distribution (SED) is shown in Figure 1a.

The true but unknown SED from an astronomical source is denoted as  $\lambda(\nu)$ , where  $\nu$  represents the frequency of the photons and  $\lambda(\nu)$  means the intensity of those arriving photons with frequency  $\nu$ . Several known templates are denoted as  $\exp(\mu_i(\nu))$ , where  $\mu_i$ 's are the template log-SEDs. The actual observation  $y_t$  we collect from the telescope is the total number of photons observed using a particular filter with a certain bandwidth  $B_t = (\nu_t - \delta_t, \nu_t + \delta_t)$ , which centers around  $\nu_t$  with a frequency range  $\delta_t$ . Let  $N_t(\cdot)$  denote the complete empirical distribution of photon arrivals emitted at time  $t$  with different frequencies. Then  $y_t = N_t(B_t)$ , because one can only observe the total counts of photons in the bandwidth  $B_t$ .

**Motivating astronomical problem.** Use all of the collected data  $y_t$ 's as well as the filters  $B_t$ 's to describe the unknown SED  $\lambda(\nu)$  in terms of the existing SED templates,  $\exp(\mu_i(\nu))$ 's.

Most existing astronomy literatures use frequentist model selection methodologies to determine which template could best represent the truth, that is, to find a unique  $i$  such that  $\lambda(\nu) = \exp(\mu_i(\nu))$ . However these methods (i) fail to quantify the uncertainty of this sole template selection away from the true SED,

(ii) cannot take advantage of such uncertainty information to suggest the next step of observational setting, and (iii) ignore the possibility that the true SED might not be accounted for by those selected templates, as shown by the region of larger  $\nu$  in Figure 1a.

To address (ii), a naive and prevailing approach for collecting observations is to use each single available filter on the telescope and fit the SED until the completion of data collection. However, this might be expensive because of the time constraint on telescope availability (on average only 8 night hours per day). Multiple visits to the telescope due to an inefficient observational strategy will increase the monetary cost for astronomers.

A unifying and adequate solution addressing all of the issues above is obtained through a Bayesian approach. Instead of choosing a sole template, we take a Bayesian model averaging perspective on those templates by assuming that  $\lambda(\nu) = \exp(\sum_{i=1}^m \omega_i \mu_i(\nu))$ , where  $\omega \triangleq (\omega_1, \dots, \omega_m)^T$  is the vector of mixture weights assigned to each template such that  $\sum_{i=1}^m \omega_i = 1$ . We summarize the existing observations as a prior distribution on  $\omega$  and accordingly induce the posterior distribution on  $\omega$  by incorporating our current observations. For (i), the uncertainty information for the goodness-of-fit of the data could be extracted from the posterior distribution on  $\omega$ , e.g., the posterior probability intervals for each  $\omega_i$ . For (ii), the posterior distribution on  $\omega$  also serves as the primary proxy for choosing the next filter to use. This is how Bayesian sequential experimental design comes into play.

Finally, to address (iii), we can write  $\lambda(\nu) = \exp(\sum_{i=1}^m \omega_i \mu_i(\nu) + \epsilon(\nu))$ , where  $\epsilon(\nu)$  describes the deviation between the true log-SED and (convex combinations of) those selected templates. Due to the limited knowledge of the unstructured term  $\epsilon(\nu)$ , we naturally impose a weak prior on it, which requires the use of a Bayesian nonparametric prior and hence motivates our study of Bayesian nonparametric sequential experimental design (BNS-ED).

### 3 Design and Inferential Scheme for BNS-ED

In this Section, we will specify the statistical models as well as the utility function for BNS-ED. We then discuss the inference for BNS-ED in general without employing any specific features of our model. The derivations of equations (2), (3), and (4) can be found in Supplementary Materials A.

#### 3.1 Model Specification

Due to the discrete nature of our observations, it is convenient to model the photon arrivals at different frequencies,  $N_t$ , as an inhomogeneous Poisson point process (or Poisson random measure):

$$N_t(\cdot) \sim {}_{|\lambda} \text{PP}(\lambda) \text{ i.i.d. for all } t,$$

$$y_t \triangleq N_t(B_t) \sim_{|B_t, \lambda} \text{Poisson} \left( \int_{B_t} \lambda(\nu) d\nu \right).$$

Also, without making any strong assumptions, it is convenient to assign the prior distribution for  $\epsilon(\nu)$ —in a nonparametric way—as a Gaussian process (GP)<sup>2</sup>:  $\epsilon(\nu) \sim \text{GP}(0, k)$ , where  $k = k(\nu, \nu')$  is the covariance function (or kernel function). In this paper, we assume that  $k$  is given, fixed, and coming from a parametric family. We can also conduct a full Bayesian inference on the parameters of  $k$  by using the inferential techniques we introduce in this paper, but for the ease of demonstration we choose not to address this point further.

Later on in the simulation we will conventionally make a stronger assumption that  $k(\nu, \nu) = \sigma^2$  for any  $\nu$ , which might not be true in practice. To have a more accurate representation of the reality about  $k$ , we can perform a maximum likelihood fitting for  $k$  from a flexible covariance structure based on existing observations. One anonymous reader also mentioned that  $\sigma^2$  should be small for observing a well-understood object, as the deviation term is essentially unnecessary. Hence, even though our Bayesian framework will allow the flexibility that the truth can deviate from the selected templates, it will also be compatible with the frequentist methodologies used by astronomers, which could provide strong predictive power for the astronomical objects.

We finally assign a prior on  $\omega$  as  $\omega \sim \text{Dir}(\alpha)$  by incorporating some astronomy prior knowledge, which we choose not to discuss here for the clarity of presentation. Another way of choosing  $\alpha$  is from an empirical moment matching on existing observations. In practice,  $m$  might be very large, so we could also choose  $\alpha$  to encourage sparse  $\omega$ .

Thus, in terms of a Bayesian graphical (or hierarchical) model representation, shown in Figure 1b, the main parameter of interest—the unknown SED  $\lambda$ —has a nonparametric prior distribution that is a log-Gaussian process with a mean function depending on  $\omega$  and a known covariance function. Levels 1–3 together specify a mixture (over  $\omega$ ) log-Gaussian Cox process (LGCP) on  $N_t(\cdot)$  (see Ghahramani et al. [2006], Lawrence and Moore [2007], Rue and Martino [2009] for its generalization), which we will use throughout this paper as the main model of interest.

### 3.2 Design Objective

Following the seminal work by Lindley [1956], we consider the expected gain in Shannon information (Shannon [1948]) as the utility function. Precisely, our design goal in BNS-ED is to sequentially choose a design that maximizes the expected Kullback-Leibler divergence between the posterior distributions of  $\omega$

---

<sup>2</sup>The choice of GP here is purely conventional. It is possible to replace this nonparametric prior by any stable process (e.g. a Cauchy process) if alternative tail behavior is desired. Our SMC approach will easily scale to such alternative specifications.

at time  $t$  and  $t - 1$ :

$$EIG_t(B_t) \triangleq \mathbb{E}_{y_t|B_t, \mathcal{F}_{t-1}} (D_{\text{KL}}(p(\omega|y_t, B_t, \mathcal{F}_{t-1}) || p(\omega|\mathcal{F}_{t-1}))), \quad (1)$$

where  $\mathcal{F}_{t-1} \triangleq \sigma(y_1, B_1, \dots, y_{t-1}, B_{t-1})$  denotes all the historical information before the  $t$ -th observation. To summarize, we want to have a series of design decisions that extract the most information for  $\omega$  after each observation.

Note that here we do not study the information gain directly on  $\lambda$  since our astronomical goal in this paper is more to analyze the unknown truth with the existing templates. We wish that the inclusion of the deviation term in some cases (like Example 2 in Section 5) can provide some signals of the existence of deviation, but, when there is no deviation, we still wish to get more information about  $\omega$ .

By using

$$p(\omega|\mathcal{F}_t) = \frac{p(y_t|B_t, \mathcal{F}_{t-1}, \omega)}{p(y_t|B_t, \mathcal{F}_{t-1})} p(\omega|\mathcal{F}_{t-1}), \quad (2)$$

the expected information gain in equation (1) can be further rewritten as

$$EIG_t(B_t) = \mathbb{E}_{\omega|\mathcal{F}_{t-1}} (D_{\text{KL}}(p(y_t|B_t, \mathcal{F}_{t-1}, \omega) || p(y_t|B_t, \mathcal{F}_{t-1}))). \quad (3)$$

The problem now reduces to approximating the expectation in equation (3), which will be approached with sequential Monte Carlo techniques.

### 3.3 Sequential Monte Carlo (SMC) Inference

We employ the SMC procedure to approximate each of the posterior distributions  $p(\omega|\mathcal{F}_{t-1})$  by a set of particles  $\{\omega_{t-1}^{(i)}, \psi_{t-1}^{(i)}\}_{i=1}^N$ . Thus, to approximate the expected information gain in equation (3), we can use

$$EIG_t(B_t) \approx \sum_{i=1}^N \psi_{t-1}^{(i)} \sum_{y_t=0}^{\infty} \log \left( \frac{p(y_t|B_t, \mathcal{F}_{t-1}, \omega_{t-1}^{(i)})}{\sum_{i'=1}^N \psi_{t-1}^{(i')} p(y_t|B_t, \mathcal{F}_{t-1}, \omega_{t-1}^{(i')})} \right) p(y_t|B_t, \mathcal{F}_{t-1}, \omega_{t-1}^{(i)}), \quad (4)$$

where the summation over  $y_t$  can be further narrowed as we describe in Subsection 4.3.

Based on this approximation, we choose  $B_t$  to maximize the approximated expected information gain from the set of available filters ( $B_t = \underset{B \in \text{Filters}}{\operatorname{argmax}} EIG_t(B)$ ). Using this filter, we acquire a new observation  $y_t$ . Then, according to equation (2), we update the particles at time  $t$  via

$$\omega_t^{(i)} = \omega_{t-1}^{(i)}, \psi_t^{(i)} \propto \psi_{t-1}^{(i)} \times p(y_t | B_t, \mathcal{F}_{t-1}, \omega_{t-1}^{(i)}),$$

for  $i = 1, \dots, N$ . Every time the particles are updated as above, we monitor the effective sample size of the particles. Once the effective sample size drops below a given threshold, we resample from the current

particles. Furthermore, in order to increase the diversity of the particles, we perturb each resampled particle by a Markovian move. To achieve this, we first note that

$$p(\omega|\mathcal{F}_t) \propto \prod_{s=1}^t p(y_s|B_s, \mathcal{F}_{s-1}, \omega) p(\omega).$$

Then, to sample from  $p(\omega|\mathcal{F}_t)$ , we just propose a new  $\omega_t^{(i),*}$  for each  $i = 1, \dots, N$  by drawing from  $\text{Dir}(\tau\omega_t^{(i)})$ , where  $\tau$  is a tuning parameter representing the step size, and then accept the proposal with the usual Metropolis-Hastings acceptance probability. Algorithm 1 in the Supplementary Materials C describes the complete methodology.

## 4 Efficient Computations for LGCP

The SMC procedure described above relies heavily on a fast and accurate way to calculate the following posterior predictive distribution for  $y_t$  using the filter  $B_t$ :

$$p(y_t|B_t, \mathcal{F}_{t-1}, \omega) = \frac{\int p(y_t|B_t, \eta) \prod_{s=1}^{t-1} p(y_s|B_s, \eta) p(\eta|\omega) d\eta}{\prod_{s=1}^{t-1} p(y_s|B_s, \mathcal{F}_{s-1}, \omega)}, \quad (5)$$

where  $\eta \triangleq \log(\lambda)$ . This might be achieved by using a vanilla Monte Carlo estimate (see Meeds and Welling [2014] for a recent development of this kind of simulation-based technique). However, due to the functional nature of a Gaussian process, the sample space in calculating equation (5) is too large for vanilla Monte Carlo integration to be computationally efficient. Furthermore, this large scale Monte Carlo estimate needs to be repeated  $N$  times for each observation time  $t$ , which clearly slows down the performance of Algorithm 1. An alternative calculation of the posterior predictive distribution will be introduced in the following two Subsections. We call this new approach the *Poisson log-normal approximation (PoLNA)* (see e.g. Adams et al. [2009] and Simpson et al. [2013] for some common ways to infer LGCP). In the third Subsection, we apply PoLNA to reduce the amount of computations needed to calculate the Kullback-Leibler divergence.

### 4.1 Poisson Log-Normal Approximation (PoLNA)

The key idea of this approximation is to reduce the dimensionality of the integral in equation (5) by finding the joint distribution of

$$\mathbf{\Lambda} = (\Lambda_1, \dots, \Lambda_t)^T \triangleq (\Lambda(B_1, \eta), \dots, \Lambda(B_t, \eta))^T \triangleq \left( \int_{B_1} e^{\eta(\nu)} d\nu, \dots, \int_{B_t} e^{\eta(\nu)} d\nu \right)^T,$$

so we will have

$$\int p(y_t|B_t, \eta) \prod_{s=1}^{t-1} p(y_s|B_s, \eta) p(\eta|\omega) d\eta = \int \text{Poisson}(y_t|\Lambda_t) \prod_{s=1}^{t-1} \text{Poisson}(y_s|\Lambda_s) p(\mathbf{\Lambda}|\omega) d\mathbf{\Lambda}.$$

Simulation studies (where a simple example for  $t = 1$  is shown in Figure 5 of Supplementary Materials B) indicate that the joint distribution of  $\log \mathbf{\Lambda}$  can be approximated by a multivariate normal distribution  $\mathcal{N}_t(\boldsymbol{\mu}_\Lambda, \boldsymbol{\Sigma}_\Lambda)$  with a high accuracy<sup>3</sup>, where  $\boldsymbol{\mu}_\Lambda$  and  $\boldsymbol{\Sigma}_\Lambda$  can be obtained either from a Monte Carlo estimate or from a deterministic numerical calculation using the extended technique of Safak [1993]. The detailed calculation for the later proposal can be found in the Supplementary Materials B.

Hence, by plugging into this approximation, the posterior predictive distribution becomes the conditional distribution of a multivariate Poisson log-normal distribution,  $\text{PLN}(\boldsymbol{\mu}, \boldsymbol{\Sigma})$ , which has a joint probability mass function

$$\text{PLN}(\mathbf{y}|\boldsymbol{\mu}, \boldsymbol{\Sigma}) = \int \prod_{s=1}^t \text{Poisson}(y_s | \Lambda_s) \mathcal{N}_t(\log \mathbf{\Lambda} | \boldsymbol{\mu}, \boldsymbol{\Sigma}) d(\log \mathbf{\Lambda}). \quad (6)$$

The (multivariate) Poisson log-normal distribution has several tractable properties such as analytical formulas for its mean vector or covariance matrix, unimodal feature, and subexponentially decaying tail. It has been studied in depth by Aitchison and Ho [1989] and Perline [1998].

## 4.2 Laplace Transform Approximation of Multivariate Log-Normal Distribution

Equation (6) is a low dimensional integral (usually there are only 10 different filters available on the telescope), so one common way to achieve this type of numerical integration is from the *multivariate Gaussian Hermite quadrature*, which does not take full advantage of the special form of the integrand—a product of several Poisson likelihoods. Thus, in this Subsection, we will introduce an alternative way to approximate equation (6) using an approximation to the Laplace transform of a multivariate log-normal distribution.

First, we rewrite (6) as

$$\text{PLN}(\mathbf{y}|\tilde{\boldsymbol{\mu}}, \tilde{\boldsymbol{\Sigma}}) = \frac{e^{\mathbf{S}^T \tilde{\boldsymbol{\Sigma}} \mathbf{S}/2 + \tilde{\boldsymbol{\mu}}^T \mathbf{S}}}{\prod_{s=1}^n \prod_{n=1}^{n_s} \tilde{y}_{sn}!} \int e^{-\mathbf{n}^T \tilde{\mathbf{\Lambda}} \log \mathcal{N}_u(\tilde{\mathbf{\Lambda}} | \tilde{\boldsymbol{\mu}} + \tilde{\boldsymbol{\Sigma}} \mathbf{S}, \tilde{\boldsymbol{\Sigma}})} d\tilde{\mathbf{\Lambda}}, \quad (7)$$

where  $\tilde{\Lambda}_s$ 's are the unique components of  $\mathbf{\Lambda}$  with corresponding multivariate log-normal parameters,  $\tilde{\boldsymbol{\mu}}$  and  $\tilde{\boldsymbol{\Sigma}}$ , and

$$\begin{aligned} \tilde{y}_{sn} &\sim_{|\tilde{\Lambda}_s} \text{Poisson}(\tilde{\Lambda}_s) \text{ i.i.d. for all } n = 1, \dots, n_s, s = 1, \dots, u; \\ \mathbf{y} &= [\tilde{y}_{sn}]_{n=1}^{n_s}{}^u_{s=1}; \mathbf{S} \triangleq \left( \sum_{n=1}^{n_1} \tilde{y}_{1n}, \dots, \sum_{n=1}^{n_u} \tilde{y}_{un} \right)^T; \mathbf{n} \triangleq (n_1, \dots, n_u)^T. \end{aligned}$$

Thus, the multivariate Poisson log-normal distribution is fully characterized by the Laplace transform of a multivariate log-normal distribution.

---

<sup>3</sup>For notation clarity, in this Subsection we allow  $\boldsymbol{\Sigma}_\Lambda$  to be degenerate, i.e., some of the  $\Lambda_s$ 's might have correlation 1.



Employing the same technique presented by Asmussen et al. [2013] (we omit the detailed proof here), we can derive a sharp approximation to the Laplace transform of a multivariate log-normal distribution as

$$\int e^{-\mathbf{n}^T \tilde{\Lambda}} \log \mathcal{N}_u \left( \tilde{\Lambda} \middle| \tilde{\boldsymbol{\mu}} + \tilde{\Sigma} \mathbf{S}, \tilde{\Sigma} \right) d\tilde{\Lambda} \approx \frac{\exp \left( -\frac{1}{2} \left( \begin{array}{c} \mathbf{W}_u(\mathbf{M})^T \tilde{\Sigma}^{-1} \mathbf{W}_u(\mathbf{M}) \\ + \mathbf{1}_u^T \tilde{\Sigma}^{-1} \mathbf{W}_u(\mathbf{M}) \end{array} \right) \right)}{\sqrt{\det(\mathbf{I}_u + \mathbf{M} \operatorname{diag}(e^{-\mathbf{W}_u(\mathbf{M})}))}}, \quad (8)$$

where  $\mathbf{M} \triangleq \tilde{\Sigma} \operatorname{diag}(\mathbf{n}) \operatorname{diag}(e^{\tilde{\boldsymbol{\mu}} + \tilde{\Sigma} \mathbf{S}})$  and  $\mathbf{W}_u(\mathbf{M})$  is the multivariate Lambert W function defined as the unique solution of  $\mathbf{M} \exp(-\mathbf{W}_u(\mathbf{M})) = \mathbf{W}_u(\mathbf{M})$ . This approximation is derived via the Laplace approximation in an asymptotic sense but it stays sharp over the entire domain of convergence of the Laplace transform. Combining equations (7) and (8) gives us an accurate and fast approximation to the multivariate Poisson log-normal distribution.

### 4.3 Efficient Calculation of Kullback-Leibler Divergence

In this Subsection, we will propose an efficient calculation scheme for equation (4) by limiting the Kullback-Leibler divergence calculations over an effective range of  $y_t$ .

For a given particle  $\boldsymbol{\omega}_{t-1}^{(i)}$  and a filter  $B_t$ , the inner summation in equation (4) can be well approximated by summing only over those  $y_t$  in the  $(1 - \alpha)$ -interval of  $p(y_t | B_t, \mathcal{F}_{t-1}, \boldsymbol{\omega}_{t-1}^{(i)})$ —thanks to the unimodal property and the subexponentially decaying tail of a Poisson log-normal distribution. We usually set  $\alpha = 5\%$ . The remaining question now is how to find these two quantiles for the conditional Poisson log-normal distribution. We will derive a pair of conservative bounds by focusing on the univariate Poisson log-normal distribution  $\text{PLN}(y_t | \mu_{tt}, \Sigma_{tt})$  since the unconditional distribution will be fatter than the conditional one.

As Perline [1998] states, the Poisson log-normal distribution has an upper tail asymptotically equal to the upper tail of the log-normal distribution, so

$$\sum_{y_t=M+1}^{\infty} \text{PLN}(y_t | \mu_{tt}, \Sigma_{tt}) \approx 1 - \Phi \left( \frac{\log M - \mu_{tt}}{\sqrt{\Sigma_{tt}}} \right). \quad (9)$$

Hence, we let the upper bound and lower bound to be

$$M_U = \left\lfloor \exp \left( z_{1-\alpha/2} \sqrt{\Sigma_{tt}} + \mu_{tt} \right) \right\rfloor + 1, \quad (10)$$

$$M_L = \left\lfloor \exp \left( z_{\alpha/2} \sqrt{\Sigma_{tt}} + \mu_{tt} \right) \right\rfloor, \quad (11)$$

where  $\lfloor x \rfloor$  means the integer part of a real number  $x$  and  $z_\alpha$  is the  $\alpha$ -quantile of a standard normal distribution.

When  $\alpha$  is small, we expect the true upper quantile for  $\text{PLN}(y_t | \mu_{tt}, \Sigma_{tt})$  to be large, so the tail approximation in equation (9) is particularly accurate, and likewise for  $M_U$  in equation (10). On the other hand,

when  $\mu_t$  is moderate, the true lower quantile is not far away from 0, which is usually the answer given by equation (11). When  $\mu_t$  is quite large, even the true lower quantile can be extreme; in this case the tail approximation in equation (9) will become accurate again, so equation (11) is still valid.

Simulation shows that both  $M_U$  and  $M_L$  offer practically useful guidance for finding the upper and lower quantiles for  $\text{PLN}(y_t|\mu_t, \Sigma_{tt})$ , which then can help us to reduce the total amount of calculations in equation (4).

## 5 Simulation

In this Section we discuss two simulation examples, one using two trigonometric templates to assess our algorithm and the other using three real templates from astronomy. Here we only focus on comparing different strategies for sequential design and demonstrating the faster speed of our methodology. The comparison between our Bayesian methodology and the existing frequentist inference methods is important but not our main focus here. Besides, those existing methods employed in astronomy community does not allow the on-line sequential learning, so neither do they have equal status to compare with our method.

In the following examples, we only study three different types of strategies<sup>4</sup>: the proposed sequential Monte Carlo strategy (SMCS) using Algorithm 1; the totally random strategy (TRS), by which the choice of the filter is totally by chance; and the greedy strategy (GS), which we deterministically choose the filters in the same order as the absolute differences between the integrated intensities  $|\Lambda(B, \mu_1) - \Lambda(B, \mu_2)|$  for different filter  $B$  and two templates  $\mu_1, \mu_2$ . Clearly, GS only works when we have two template models. We note that TRS and GS are indeed the current methodologies employed by astronomers.

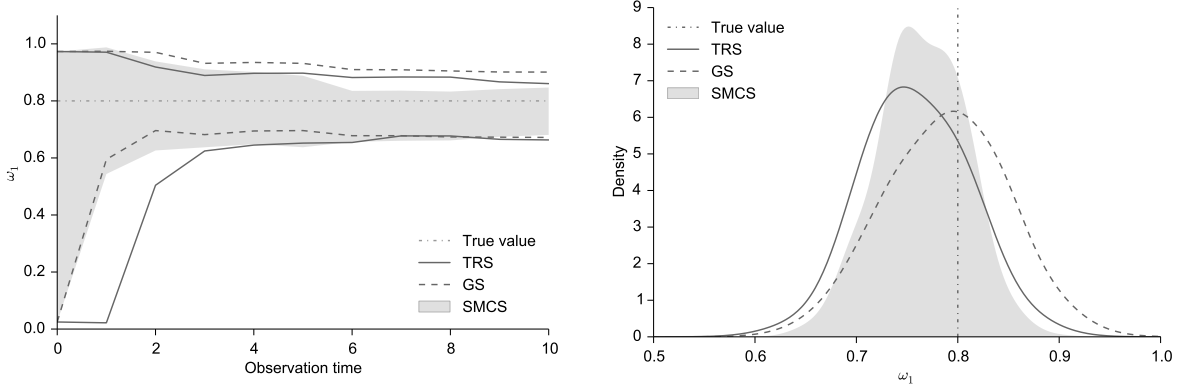
This simulation section is primarily an illustration, for the real data includes more domain-specific technicalities and will affect the clarity of our presentation. These empirical results will be included in a follow-up paper. Note that the outcomes and takeaways are similar for the real data as for the simulation—SMCS will clearly perform better than the TRS, which is commonly used in astronomy. Hence, the primary change in the real setting will be to include a larger template base (over 100 templates), but our methodology can easily adapt to this much more complicate setting.

**Example 1: Exponential Trigonometric Templates** We use two templates ( $m = 2$ ) and let

$$\begin{aligned}\eta_{\text{true}}(\nu) &= \log(\lambda_{\text{true}}(\nu)) = \omega_{1,\text{true}}\mu_1(\nu) + \omega_{2,\text{true}}\mu_2(\nu), \quad \boldsymbol{\omega}_{\text{true}} = (0.8, 0.2)^T, \\ \mu_1(\nu) &= 2 \sin(2\pi\nu) + 4, \quad \mu_2(\nu) = 2 \cos(2\pi\nu) + 4, \quad \nu \in [0, 1],\end{aligned}$$

---

<sup>4</sup>One anonymous reader once suggested to add the comparison with GP-UCB strategy proposed by Srinivas et al. [2010] in our simulation, but, as discussed in Section 6.1, their setting is different from our work here and hence GP-UCB is not directly applicable.



(a) 95% posterior probability interval of  $\omega_1$ .

(b) Posterior density of  $\omega_1$  at  $t = 10$ .

Figure 2: A time-varying demonstration for the posterior distribution of  $\omega_1$  for Example 1.

$$k(\nu, \nu') = \sigma^2 \exp\left(-\frac{(\nu - \nu')^2}{2l^2}\right), \quad \sigma = 0.2, \quad l = 0.02,$$

and finally let the range of  $y_t$  for calculating equation (4) come from (10) and (11). The ten filters available here have frequency range  $[0, 0.1]$ ,  $[0.1, 0.2]$ , ...,  $[0.9, 1]$ . For each strategy (TRS, GS, and SMCS), we run the simulation up to  $t = 10$ .

The 95% posterior probability intervals of  $\omega_1$  for each time  $t$  can be found in Figure 2a. The probability interval of  $\omega_1$  at  $t = 0$  comes from the uniform prior on  $[0, 1]$ . Both SMC and GS converge faster and give narrower intervals (since  $t = 1$ ) than TRS. Figure 2b also shows that both SMCS and GS give a narrower and less biased result than TRS. In this case, SMCS performs slightly better than GS in terms of the root of posterior mean square error (6.6% for TRS, 6.0% for GS, and 5.5% for SMCS). Recall that GS is valid only when  $m = 2$ , but the proposed SMCS can be applied to other cases. Actually, the generalization of GS for the case of  $m > 2$  is our very first motivation to study this work.

**Example 2: Active Galactic Nuclei (AGN), Composite (COMP), and Starburst (SB) Templates** In this example, we set  $m = 3$  and use three real templates from astronomy: AGN NGC5506, COMP IRAS 19254-7245, and SB NGC 7714 (Richards et al. [2006], Elvis et al. [1994], Hopkins et al. [2007]). The frequency is scaled to  $[0, 1]$  with the set of filters being the same as in Example 1. Now let

$$\eta_{\text{true}}(\nu) = \omega_{1,\text{true}}\mu_{\text{AGN}}(\nu) + \omega_{2,\text{true}}\mu_{\text{COMP}}(\nu) + \omega_{3,\text{true}}\mu_{\text{SB}}(\nu).$$

The shape of  $\mu_{\text{AGN}}$ ,  $\mu_{\text{COMP}}$  and  $\mu_{\text{SB}}$  can be found in Figure 4a. We consider two cases to demonstrate the importance of including a Gaussian process (GP) component in the modelling of the unknown  $\eta(\nu)$ .

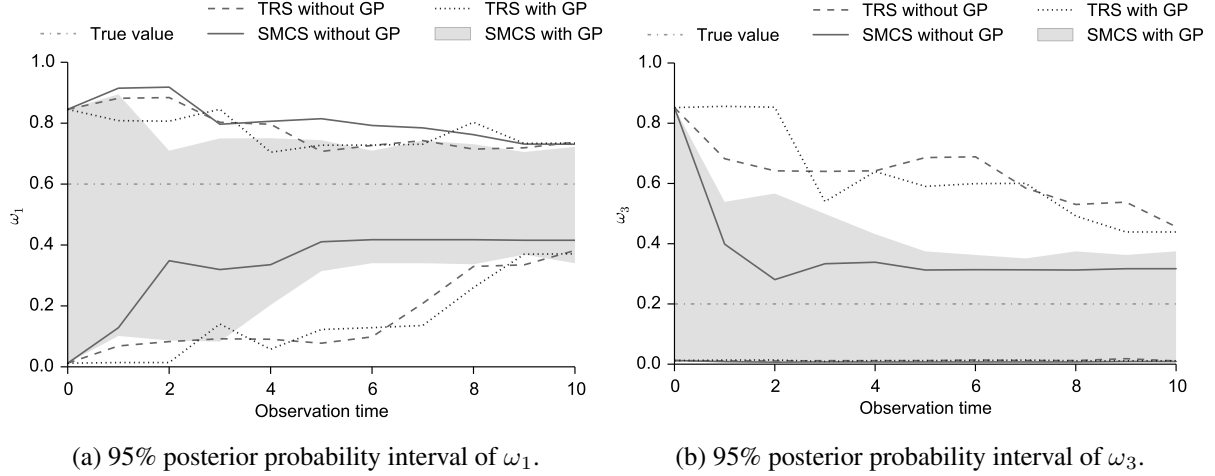


Figure 3: A time-varying demonstration for the posterior distribution of  $\omega$  in the Case 1 of Example 2.

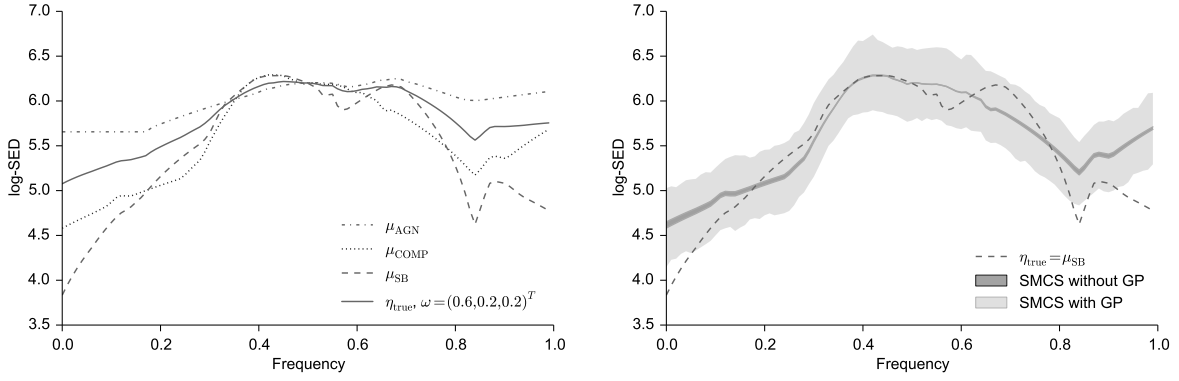
**Case 1: Correctly specified templates.** Let  $\omega_{\text{true}} = (0.6, 0.2, 0.2)^T$  and use all the three templates ( $\mu_{\text{AGN}}$ ,  $\mu_{\text{COMP}}$ , and  $\mu_{\text{SB}}$ ) for estimation.  $\eta_{\text{true}}$  in this case is also plotted in Figure 4a. We compare SMCS and TRS under two scenarios: modelling  $\eta$  with a GP prior and without a GP prior. For the first scenario, we choose  $k$  the same as in Example 1. The 95% posterior probability intervals of  $\omega_1$  and  $\omega_3$  are shown in Figure 3. SMCS without a GP prior results in the narrowest interval because  $\eta_{\text{true}}$  is correctly specified by the templates. On the other hand, no matter whether a GP prior is used or not, SMCS converges faster than the TRS.

Here we emphasize that the slow convergence in Figure 3 does not come from the approximation error of PoLNA (as the two cases without GP does not require any approximation) but instead from the small differences of the integrated intensities (for each filter) among the templates. It seems that the three templates differ significantly in Figure 4a, but their actual integrated intensities do not.

**Case 2: Misspecified templates.** Now we let  $\omega_{\text{true}} = (0, 0, 1)^T$ , so  $\eta_{\text{true}} = \mu_{\text{SB}}$ . In this case, we only use  $\mu_{\text{AGN}}$  and  $\mu_{\text{COMP}}$  for estimation, so any simple convex combinations of  $\mu_{\text{AGN}}$  and  $\mu_{\text{COMP}}$  are still far away from the truth. We compare the SMCS with and without a GP prior using the same  $k$  as in Example 1, and in Figure 4b we plot the 95% posterior region of  $\eta$  at  $t = 10$  (marginally for each  $\nu$ ). SMCS with a GP prior outperforms SMCS without a GP prior, because the posterior region of the former is more capable of covering  $\eta_{\text{true}}$ . Precisely, with a GP prior on  $\eta$  there is a 27% posterior probability that

$$\|\eta - \eta_{\text{true}}\|_{\infty} \leq \|\mu_{\text{COMP}} - \eta_{\text{true}}\|_{\infty},$$

where  $\|f\|_{\infty} \triangleq \sup \{|f(\nu)| : \nu \in [0, 1]\}$  and  $\mu_{\text{COMP}}$  is the most achievable estimation of  $\eta$  without using a GP prior. A GP prior on  $\eta$  allows more adaptation to the data, which leads to a more reliable conclusion—



(a) The three real templates from the astronomy. Also (b) 95% posterior region of  $\eta$  when  $t = 10$  in the Case shown here is  $\eta_{\text{true}}$  we study in the Case 1. 2.

Figure 4: Illustrations of Example 2 in terms of log-SED's.

even though the templates we use for estimation cannot completely describe the truth. This proves the potential and the practical value of our methodology.

## 6 Discussion

### 6.1 Differences with related works

**Bayesian experimental design versus Bayesian optimization.** The use of Gaussian process (GP) to sequentially choose the next experiment to perform so as to optimize some value of information can be traced back to Kushner [1963]. The research along this line is generally called *Bayesian optimization*. More literature reviews in this direction can be found in the survey papers Brochu et al. [2010] and Frazier [2010]. In this context, Villemonteix et al. [2009] also uses an information theoretic criterion similar to our work.

However, our formulation of Bayesian sequential experimental design is fundamentally different from Bayesian optimization. Optimization aims to find the optimum of a given target (a local criterion); experimental design seeks to characterize the entire target distribution (a global criterion), as measured by some (set of) aggregate information metric(s). Hence, the focus of our approach is not the same as those Bayesian optimization literatures.

**Sequential design versus non-sequential design.** There are indeed some literatures study experimental design with global criterion using the Bayesian nonparametric GP prior. For example, Sacks et al. [1989] seeks to minimize integrated mean square error, while Shewry and Wynn [1987] and Currin et al. [1991] want to maximize the entropy of the posterior. However, these papers do not study the sequential procedure, so they are different from our paper.

As far as we know, only few existing papers aim to *globally* understand a target, studying *sequential* design and *Bayesian nonparametric* estimation at the same time, which is what we have done in this paper. The most matchable literature we know so far regarded to the intersection between Bayesian nonparametrics and Bayesian sequential experimental design is Ferreira and Sanyal [2014], which still differs a lot from our work not only in the scientific goal, in the design problem formulation, but also in the inferential techniques.

**Non-conjugate model versus Gaussian conjugate model.** Even though Ferreira and Sanyal [2014] is the most similar literature to our work so far, they consider only the *conjugate* GP model with continuous Gaussian measurement error for the observations. Actually, most of the existing GP literatures (whether focusing on Bayesian optimization, active learning, or other problems) assume the Gaussian conjugacy in their model setting, in which case the inference techniques are still based on closed analytical forms.

However, our approach is capable of dealing with *non-conjugate* Bayesian nonparametric models. Our paper not only adopts a non-conjugate normal-Poisson model but also provides an efficient inference technique (SMC) that can generalize to other nonparametric priors. Even though Gramacy and Polsona [2011] also study SMC inference for the sequential design on a GP, they neither focus on a global criterion to understand the target nor use a non-conjugate model.

**Design versus inference in the non-conjugate hierarchical Bayesian nonparametric model.** Our paper studies sequential active learning in addition to performing inference in a non-conjugate hierarchical Bayesian nonparametric model. While many papers have studied the inference portion of this task (usually based on LGCP, such as Rue and Martino [2009] and Simpson et al. [2013]), none have simultaneously tackled the design problem, largely due to the huge computational cost. In this paper, we have created an efficient computational approach to solve this problem, demonstrating its usefulness on an astronomical application.

## 6.2 Conclusion

In this paper, we first study the problem of Bayesian nonparametric sequential experimental design (BNS-ED) without conjugacy. We build a three-level hierarchical Bayesian nonparametric model that aims to find the optimal astronomical observational strategy. A sequential Monte Carlo (SMC) strategy is then proposed to solve the problem of interest. To overcome the computation hurdle inherited naturally from the log-Gaussian Cox process (LGCP), we exploit the special features of this model and provide a new inference technique for it, called Poisson log-normal approximation (PoLNA), which can still be applied even for spatial-temporal LGCP.

We would like to emphasize that even though we mainly focus on the widely studied LGCP in this paper, the BNS-ED framework we discuss here and the corresponding inferential scheme, which employs sequential Monte Carlo techniques, can be easily generalized to other nonparametric models.

The computation problem encountered in this paper is generally difficult, so we suspect that this is why there is no existing work on this topic—sequential design for globally learning a nonparametric target with non-conjugate sampling distribution. Our computational technique provides the algorithmic speed to make this idea practical on real applications, which then justifies the novelty and value of our approach.

## References

- R. P. Adams, I. Murray, and D. J. MacKay. Tractable nonparametric bayesian inference in poisson processes with gaussian process intensities. In *Proceedings of the 26th International Conference on Machine Learning*, pages 9–16, Montreal, 2009.
- J. Aitchison and C. H. Ho. The multivariate poisson-log normal distribution. *Biometrika*, 76(4):643–653, December 1989.
- S. Asmussen, J. L. Jensen, and L. Rojas-Nandayapa. On the laplace transform of the lognormal distribution. *Thiele centre preprint*, 2013.
- D. A. Berry and B. Fristedt, editors. *Bandit Problems: Sequential Allocation of Experiments*. Chapman and Hall, London, 1985.
- E. Brochu, V. M. Cora, and N. de Freitas. A tutorial on bayesian optimization of expensive cost functions, with application to active user modeling and hierarchical reinforcement learning. arXiv:1012.2599, December 2010. Unpublished manuscript.
- K. Chaloner and I. Verdinelli. Bayesian experimental design: A review. *Statistical Science*, 10(3):273–304, 1995.
- M. Cherkassky and L. Bornn. Sequential monte carlo bandits. ArXiv: 1310.1404, October 2013. Unpublished manuscript.
- C. Currin, T. Mitchell, M. Morris, and Y. Don. Bayesian prediction of deterministic functions, with applications to the design and analysis of computer experiments. *Journal of the American Statistical Association*, 86(416):953–963, December 1991.
- M. Elvis, B. J. Wilkes, J. C. McDowell, R. F. Green, J. Bechtold, S. P. Willner, M. S. Oey, E. Polonski, and R. Cutri. Atlas of quasar energy distributions. *ApJS*, 95:1–68, Nov. 1994. doi: 10.1086/192093.
- M. A. R. Ferreira and N. Sanyal. Bayesian optimal sequential design for nonparametric regression via inhomogeneous evolutionary mcmc. *Statistical Methodology*, 18:131–141, 2014.
- P. I. Frazier. Decision-theoretic foundations of simulation optimization. *Wiley Encyclopedia of Operations Research and Management Science*, 2010.
- Z. Ghahramani, T. L. Griffiths, and P. Sollich. Bayesian nonparametric latent feature models. In *Proceedings of the 8th Valencia International Meetings on Bayesian Statistics*, June 2006.
- R. B. Gramacy and N. G. Polsona. Particle learning of gaussian process models for sequential design and optimization. *Journal of Computational and Graphical Statistics*, 20(1):102–118, 2011.
- P. F. Hopkins, G. T. Richards, and L. Hernquist. An Observational Determination of the Bolometric Quasar Luminosity Function. *ApJ*, 654:731–753, Jan. 2007. doi: 10.1086/509629.

- C.-W. Ko, J. Lee, and M. Queyranne. An exact algorithm for maximum entropy sampling. *Operations Research*, 43(4):684–691, July 1995.
- A. Krause and C. S. Ong. Contextual gaussian process bandit optimization. In J. Shawe-Taylor, R. Zemel, P. Bartlett, F. Pereira, and K. Weinberger, editors, *Advances in Neural Information Processing Systems 24*, pages 2447–2455, 2011.
- H. J. Kushner. A new method of locating the maximum of an arbitrary multi-peak curve in the presence of noise. *Journal of Fluids Engineering*, 86(1):97–106, March 1963.
- N. D. Lawrence and A. J. Moore. Hierarchical gaussian process latent variable models. In *Proceedings of the 24th International Conference on Machine Learning*, 2007.
- D. V. Lindley. On the measure of information provided by an experiment. *Annals of Statistics*, 27:986–1005, 1956.
- E. Meeds and M. Welling. Gps-abc: Gaussian process surrogate approximate bayesian computaiton. ArXiv:1401.2838, January 2014. Unpublished manuscript.
- R. Perline. Mixed poisson distributions tail equivalent to their mixing distributions. *Statistics & Probability Letters*, 38(3):229–233, June 1998.
- G. T. Richards et al. Spectral Energy Distributions and Multiwavelength Selection of Type 1 Quasars. *ApJS*, 166:470–497, Oct. 2006. doi: 10.1086/506525.
- H. E. Robbins. Some aspects of the sequential design of experiments. *Bulletin of the American Mathematical Society*, 58(5):527–535, 1952. doi: doi:10.1090/S0002-9904-1952-09620-8.
- H. Rue and S. Martino. Approximate bayesian inference for latent gaussian models by using integrated nested laplace approximations. *Journal of the Royal Statistical Society: Series B (Statistical Methodology)*, 71(2):319–392, 2009.
- J. Sacks, S. B. Schiller, and W. J. Welch. Design for computer experiments. *Technometrics*, 31(1):41–47, February 1989.
- A. Safak. Statistical analysis of the power sum of multiple correlated log-normal components. *IEEE Transactions on Vehicular Technology*, 42(1):58–61, February 1993.
- C. E. Shannon. A mathematical theory of communication. *The Bell System Technical Journal*, 27:379–423, 623–656, July, October 1948.
- M. C. Shewry and H. P. Wynn. Maximum entropy sampling. *Journal of Applied Statistics*, (14):165–170, 1987.
- D. Simpson, J. B. Illian, F. Lindgren, S. H. Sørbye, and R. Hävard. Going off grid: Computationally efficient inference for log-gaussian cox processes. ArXiv:1111.0641, December 2013. Unpublished manuscript.
- N. Srinivas, A. Krause, S. Kakade, and M. Seeger. Gaussian process optimization in the bandit setting: No regret and experimental design. In *Proceedings of the 27th International Conference on Machine Learning*, 2010.
- J. Villemonteix, E. Vazquez, and E. Walter. An informational approach to the global optimization of expensive-to-evaluate functions. *Journal of Global Optimization*, 2009.

## A Derivations

### A.1 Equation (2)

By Bayes Theorem,

$$p(\omega|y_t, B_t, \mathcal{F}_{t-1}) = \frac{p(y_t, B_t|\omega, \mathcal{F}_{t-1}) p(\omega|\mathcal{F}_{t-1})}{p(y_t, B_t|\mathcal{F}_{t-1})} = \frac{p(y_t|B_t, \omega, \mathcal{F}_{t-1}) p(B_t|\omega, \mathcal{F}_{t-1}) p(\omega|\mathcal{F}_{t-1})}{p(y_t, B_t|\mathcal{F}_{t-1})}$$



$$= \frac{p(y_t|B_t, \omega, \mathcal{F}_{t-1}) p(B_t|\mathcal{F}_{t-1}) p(\omega|\mathcal{F}_{t-1})}{p(y_t, B_t|\mathcal{F}_{t-1})} = \frac{p(y_t|B_t, \omega, \mathcal{F}_{t-1})}{p(y_t|B_t, \mathcal{F}_{t-1})} p(\omega|\mathcal{F}_{t-1}),$$

where the third line follows from  $p(B_t|\omega, \mathcal{F}_{t-1}) = p(B_t|\mathcal{F}_{t-1})$  because by definition  $B_t$  and  $\omega$  are independent given  $\mathcal{F}_{t-1}$ .

## A.2 Equation (3)

Let us simplify the expected information gain  $EIG_t(B_t)$  in equation (1). We note that

$$\begin{aligned} D_{\text{KL}}(p(\omega|y_t, B_t, \mathcal{F}_{t-1}) || p(\omega|\mathcal{F}_{t-1})) &= \int \log \left( \frac{p(\omega|y_t, B_t, \mathcal{F}_{t-1})}{p(\omega|\mathcal{F}_{t-1})} \right) p(\omega|y_t, B_t, \mathcal{F}_{t-1}) d\omega \\ &= \int \log \left( \frac{p(y_t|B_t, \omega, \mathcal{F}_{t-1})}{p(y_t|B_t, \mathcal{F}_{t-1})} \right) \frac{p(y_t|B_t, \omega, \mathcal{F}_{t-1})}{p(y_t|B_t, \mathcal{F}_{t-1})} p(\omega|\mathcal{F}_{t-1}) d\omega, \end{aligned}$$

where the second line follows from equation (2). Therefore, by swapping the integral and the summation,

$$\begin{aligned} EIG_t(B_t) &= \sum_{y_t=0}^{\infty} D_{\text{KL}}(p(\omega|y_t, B_t, \mathcal{F}_{t-1}) || p(\omega|\mathcal{F}_{t-1})) p(y_t|B_t, \mathcal{F}_{t-1}) \\ &= \int \sum_{y_t=0}^{\infty} \log \left( \frac{p(y_t|B_t, \omega, \mathcal{F}_{t-1})}{p(y_t|B_t, \mathcal{F}_{t-1})} \right) p(y_t|B_t, \omega, \mathcal{F}_{t-1}) p(\omega|\mathcal{F}_{t-1}) d\omega \\ &= \mathbb{E}_{\omega|\mathcal{F}_{t-1}} (D_{\text{KL}}(p(y_t|B_t, \omega, \mathcal{F}_{t-1}) || p(y_t|B_t, \mathcal{F}_{t-1}))). \end{aligned}$$

## A.3 Equation (5)

Recall that

$$\begin{aligned} p(y_t|B_t, \mathcal{F}_{t-1}, \omega) &= \frac{p(y_t, B_t|\mathcal{F}_{t-1}, \omega)}{p(B_t|\mathcal{F}_{t-1}, \omega)} = \frac{\int p(y_t, B_t|\mathcal{F}_{t-1}, \eta, \omega) p(\eta|\mathcal{F}_{t-1}, \omega) d\eta}{p(B_t|\mathcal{F}_{t-1}, \omega)} \\ &= \frac{\int (p(y_t|B_t, \mathcal{F}_{t-1}, \eta, \omega) p(B_t|\mathcal{F}_{t-1}, \eta, \omega) p(\eta|\mathcal{F}_{t-1}, \omega)) d\eta}{p(B_t|\mathcal{F}_{t-1}, \omega)} \\ &= \int p(y_t|B_t, \eta) p(\eta|\mathcal{F}_{t-1}, \omega) d\eta, \end{aligned}$$

and

$$\begin{aligned} p(\eta|\mathcal{F}_{t-1}, \omega) &= \frac{p(y_{t-1}, B_{t-1}|\eta, \mathcal{F}_{t-2}, \omega) p(\eta|\mathcal{F}_{t-2}, \omega)}{p(y_{t-1}, B_{t-1}|\mathcal{F}_{t-2}, \omega)} \\ &= \frac{p(y_{t-1}|B_{t-1}, \eta, \mathcal{F}_{t-2}, \omega) p(B_{t-1}|\mathcal{F}_{t-2}, \omega) p(\eta|\mathcal{F}_{t-2}, \omega)}{p(y_{t-1}|B_{t-1}, \mathcal{F}_{t-2}, \omega) p(B_{t-1}|\mathcal{F}_{t-2}, \omega)} \\ &= \frac{p(y_{t-1}|B_{t-1}, \eta) p(\eta|\mathcal{F}_{t-2}, \omega)}{p(y_{t-1}|B_{t-1}, \mathcal{F}_{t-2}, \omega)} = \dots = \frac{\prod_{s=1}^{t-1} p(y_s|B_s, \eta)}{\prod_{s=1}^{t-1} p(y_s|B_s, \mathcal{F}_{s-1}, \omega)} p(\eta|\omega). \end{aligned}$$

Combining the two formulas above will give us equation (5).

#### A.4 Equation (7)

We have

$$\begin{aligned}
\text{PLN}(\mathbf{y}|\tilde{\boldsymbol{\mu}}, \tilde{\boldsymbol{\Sigma}}) &= \int \left( \prod_{s=1}^u \prod_{n=1}^{n_s} \text{Poisson}(\tilde{y}_{sn} | \tilde{\Lambda}_s) \mathcal{N}_u(\log \tilde{\Lambda} | \tilde{\boldsymbol{\mu}}, \tilde{\boldsymbol{\Sigma}}) \right) d(\log \tilde{\Lambda}) \\
&= \frac{\det(2\pi \tilde{\boldsymbol{\Sigma}})^{-1/2}}{\prod_{s=1}^n \prod_{n=1}^{n_s} \tilde{y}_{sn}!} \int e^{-\mathbf{n}^T e^{\mathbf{x}} + \mathbf{S}^T \mathbf{x}} e^{-(\mathbf{x} - \tilde{\boldsymbol{\mu}})^T \tilde{\boldsymbol{\Sigma}}^{-1} (\mathbf{x} - \tilde{\boldsymbol{\mu}})/2} d\mathbf{x} \\
&= \frac{\det(2\pi \tilde{\boldsymbol{\Sigma}})^{-1/2} e^{(\tilde{\boldsymbol{\mu}} + \tilde{\boldsymbol{\Sigma}} \mathbf{S})^T \tilde{\boldsymbol{\Sigma}}^{-1} (\tilde{\boldsymbol{\mu}} + \tilde{\boldsymbol{\Sigma}} \mathbf{S})/2 - \tilde{\boldsymbol{\mu}}^T \tilde{\boldsymbol{\Sigma}}^{-1} \tilde{\boldsymbol{\mu}}/2}}{\prod_{s=1}^n \prod_{n=1}^{n_s} \tilde{y}_{sn}!} \\
&\quad \times \int e^{-\mathbf{n}^T e^{\mathbf{x}}} e^{-(\mathbf{x} - \tilde{\boldsymbol{\mu}} - \tilde{\boldsymbol{\Sigma}} \mathbf{S})^T \tilde{\boldsymbol{\Sigma}}^{-1} (\mathbf{x} - \tilde{\boldsymbol{\mu}} - \tilde{\boldsymbol{\Sigma}} \mathbf{S})/2} d\mathbf{x} \\
&= \frac{e^{\mathbf{S}^T \tilde{\boldsymbol{\Sigma}} \mathbf{S}/2 + \tilde{\boldsymbol{\mu}}^T \mathbf{S}}}{\prod_{s=1}^n \prod_{n=1}^{n_s} \tilde{y}_{sn}!} \int e^{-\mathbf{n}^T \tilde{\Lambda}} \log \mathcal{N}_u(\tilde{\Lambda} | \tilde{\boldsymbol{\mu}} + \tilde{\boldsymbol{\Sigma}} \mathbf{S}, \tilde{\boldsymbol{\Sigma}}) d\tilde{\Lambda},
\end{aligned}$$

where  $\tilde{\Lambda}_s$ 's are the unique components of  $\Lambda$  with corresponding multivariate log-normal parameters being  $\tilde{\boldsymbol{\mu}}$  and  $\tilde{\boldsymbol{\Sigma}}$  and

$$\begin{aligned}
\tilde{y}_{sn} | \tilde{\Lambda}_s &\sim \text{Poisson}(\tilde{\Lambda}_s) \text{ i.i.d. for all } n = 1, \dots, n_s, s = 1, \dots, u; \\
\mathbf{y} &= [\tilde{y}_{sn}]_{n=1}^{n_s}{}_{s=1}^u; \mathbf{S} \triangleq \left( \sum_{n=1}^{n_1} \tilde{y}_{1n}, \dots, \sum_{n=1}^{n_u} \tilde{y}_{un} \right)^T; \\
\mathbf{n} &\triangleq (n_1, \dots, n_u)^T; \mathbf{x} \triangleq (\log \tilde{\Lambda}_1, \dots, \log \tilde{\Lambda}_u)^T.
\end{aligned}$$

## B PoLNA Parameters Calculation

In this Section, we will introduce the detailed procedures to calculate  $\boldsymbol{\mu}_\Lambda$  and  $\boldsymbol{\Sigma}_\Lambda$ . After a fine discretization on the frequency space ( $\nu$ ), we will have

$$\begin{aligned}
\boldsymbol{\eta} &\sim \mathcal{N}_D(\boldsymbol{\mu}_\eta, \mathbf{K}), [\boldsymbol{\eta}]_j \triangleq \eta(\nu^{(j)}), \\
[\boldsymbol{\mu}_\eta]_j &\triangleq \sum_{i=1}^m \omega_i \mu_i(\nu^{(j)}), [\mathbf{K}]_{j,j'} \triangleq \left[ k(\nu^{(j')}, \nu^{(j)}) \right], \quad j, j' = 1, \dots, D, \\
\Lambda(B, \eta) &\approx \sum_{\nu^{(j)} \in B} e^{\eta(\nu^{(j)})} (\nu^{(j)} - \nu^{(j-1)}).
\end{aligned}$$

$D$  is the number of discretization.

The distribution of  $\Lambda(B, \eta)$  is approximated by a log-normal distribution. We have

$$\log(\Lambda(B, \eta)) = \log \left( \sum_{\nu^{(j)} \in B} e^{\eta(\nu^{(j)})} (\nu^{(j)} - \nu^{(j-1)}) \right) = \log \left( \sum_{\nu^{(j)} \in B} e^{\eta(\nu^{(j)}) + \log(\nu^{(j)} - \nu^{(j-1)})} \right).$$

Also,  $\eta(\nu^{(j)}) + \log(\nu^{(j)} - \nu^{(j-1)})$  follows a multivariate normal distribution. Our problem now is equal to the following one:

$$(y_1^1, \dots, y_{n_1}^1, \dots, y_1^m, y_{n_m}^m) \sim \mathcal{N}_n(\boldsymbol{\mu}_y, \boldsymbol{\Sigma}_y)$$

Here,  $n = \sum_{i=1}^m n_i$ . Let  $s^i = \log\left(\sum_{j=1}^{n_i} e^{y_j^i}\right)$ . Approximately,

$$(s^1, \dots, s^m) \sim \mathcal{N}_m(\boldsymbol{\mu}_s, \boldsymbol{\Sigma}_s)$$

For all  $i, 1 \leq k \leq n_i$ , define  $s_k^i = \sum_{j=1}^k y_j^i$ , so  $s_{n_i}^i = s^i$ . Then

$$s_k^i = \log(e^{s_{k-1}^i} + e^{y_k^i}) = s_{k-1}^i + \log(1 + e^{w_k^i})$$

where  $w_k^i = y_k^i - s_{k-1}^i$ .

For any two random variables  $X$  and  $Y$ , let  $\mu_X \triangleq \mathbb{E}(X)$ ,  $\sigma_X^2 \triangleq \text{Var}(X)$ , and  $\rho_{XY} \triangleq \text{Cor}(X, Y)$ .

Following Safak [1993], we have

$$\begin{aligned} \mu_{s_k^i} &= \mu_{s_{k-1}^i} + G_1(\sigma_{w_k^i}, \mu_{w_k^i}) \\ \mu_{w_k^i} &= \mu_{y_k^i} - \mu_{s_{k-1}^i} \\ \sigma_{w_k^i}^2 &= \sigma_{y_k^i}^2 - \sigma_{s_{k-1}^i}^2 - 2\rho_{s_{k-1}^i, y_k^i} \sigma_{y_k^i} \sigma_{s_{k-1}^i} \\ \sigma_{s_k^i}^2 &= \sigma_{s_{k-1}^i}^2 - G_1^2(\sigma_{w_k^i}, \mu_{w_k^i}) + G_2(\sigma_{w_k^i}, \mu_{w_k^i}) + 2\frac{\sigma_{s_{k-1}^i}^2}{\sigma_{w_k^i}^2} (\rho_{s_{k-1}^i, y_k^i} \sigma_{y_k^i} - \sigma_{s_{k-1}^i}) G_3(\sigma_{w_k^i}, \mu_{w_k^i}) \\ \rho_{s_j^i, y_k^i} &= \rho_{s_{j-1}^i, y_k^i} \frac{\sigma_{s_{j-1}^i}}{\sigma_{s_j^i}} \left(1 - \frac{G_3(\sigma_{w_j^i}, \mu_{w_j^i})}{\sigma_{w_j^i}^2}\right) + \rho_{y_j^i, y_k^i} \frac{\sigma_{y_j^i}}{\sigma_{s_j^i} \sigma_{w_j^i}^2} \frac{G_3(\sigma_{w_j^i}, \mu_{w_j^i})}{\sigma_{w_j^i}^2}, \end{aligned}$$

where  $G_1$ ,  $G_2$ , and  $G_3$  will be defined later.

We have two methods to compute  $\rho_{s_{n_i}^i, s_{n_j}^j}$ . For any  $i, j$  and  $1 \leq k_1 \leq n_i - 1, 1 \leq k_2 \leq n_j - 1$ , suppose we already know  $\rho_{s_{k_1}^i, s_{k_2}^j}$ . Then we could first update  $\rho_{s_{k_1+1}^i, s_{k_2}^j}$  and then  $\rho_{s_{k_1+1}^i, s_{k_2+2}^j}$ . The strategy is as follows:

$$\mathbb{E}\left(s_{k_2}^j - \mu_{s_{k_2}^j} \middle| w_{k_1+1}^i\right) = \frac{\rho_{w_{k_1+1}^i, s_{k_2}^j} \sigma_{s_{k_2}^j}}{\sigma_{w_{k_1+1}^i}} (w_{k_1+1}^i - \mu_{w_{k_1+1}^i}),$$

where

$$\begin{aligned} \rho_{s_{k_1+1}^i, s_{k_2}^j} &= \frac{\mathbb{E}\left(\left(s_{k_1}^i - \mu_{s_{k_1}^i} + \log(1 + e^{w_{k_1+1}^i})\right) \left(s_{k_2}^j - \mu_{s_{k_2}^j}\right)\right)}{\sigma_{s_{k_1+1}^i} \sigma_{s_{k_2}^j}} \\ &= \rho_{s_{k_1}^i, s_{k_2}^j} \frac{\sigma_{s_{k_1}^i}}{\sigma_{s_{k_1+1}^i}} + \rho_{w_{k_1+1}^i, s_{k_2}^j} \frac{G_3(\sigma_{w_{k_1+1}^i}, \mu_{w_{k_1+1}^i})}{\sigma_{s_{k_1+1}^i} \sigma_{w_{k_1+1}^i}}. \end{aligned}$$

We could have similar formulas for  $\rho_{s_{k_1+1}^i, s_{k_2+2}^j}$ .

For a special case, if we have  $n_i = n_j$  and already know  $\rho_{s_k^i, s_k^j}$ ,  $1 \leq k \leq n_i - 1 = n_j - 1$ , we will have

$$\begin{aligned} \rho_{s_{k+1}^i, s_{k+1}^j} &= \frac{\mathbb{E} \left( \begin{pmatrix} s_k^i - \mu_{s_k^i} + \log(1 + e^{w_{k+1}^i}) \\ -G_1(\sigma_{w_{k+1}^i}, \mu_{w_{k+1}^i}) \end{pmatrix} \begin{pmatrix} s_k^j - \mu_{s_k^j} + \log(1 + e^{w_{k+1}^j}) \\ -G_1(\sigma_{w_{k+1}^j}, \mu_{w_{k+1}^j}) \end{pmatrix} \right)}{\sigma_{s_{k+1}^i} \sigma_{s_{k+1}^j}} \\ &= \rho_{s_k^i, s_k^j} \frac{\sigma_{s_k^i} \sigma_{s_k^j}}{\sigma_{s_{k+1}^i} \sigma_{s_{k+1}^j}} + \rho_{w_{k+1}^i, s_k^j} \frac{\sigma_{s_k^j} G_3(\sigma_{w_{k+1}^i}, \mu_{w_{k+1}^i})}{\sigma_{s_{k+1}^i} \sigma_{s_{k+1}^j} \sigma_{w_{k+1}^i}} + \rho_{w_{k+1}^j, s_k^i} \frac{\sigma_{s_k^i} G_3(\sigma_{w_{k+1}^j}, \mu_{w_{k+1}^j})}{\sigma_{s_{k+1}^j} \sigma_{s_{k+1}^i} \sigma_{w_{k+1}^j}} \\ &\quad + \frac{\mathbb{E} \left( \log(1 + e^{w_{k+1}^i}) \log(1 + e^{w_{k+1}^j}) \right) - G_1(\sigma_{w_{k+1}^i}, \mu_{w_{k+1}^i}) G_1(\sigma_{w_{k+1}^j}, \mu_{w_{k+1}^j})}{\sigma_{s_{k+1}^i} \sigma_{s_{k+1}^j}}, \end{aligned}$$

where  $\mathbb{E} \left( \log(1 + e^{w_{k+1}^i}) \log(1 + e^{w_{k+1}^j}) \right)$  could be computed with Gauss-Hermite quadrature.

We have

$$\begin{aligned} F(\sigma, m, k) &\triangleq e^{-km + \frac{k^2 \sigma^2}{2}} \Phi\left(\frac{m - k\sigma^2}{\sigma}\right), \\ \Phi(x) &\triangleq \frac{1}{\sqrt{2\pi}} \int_{-\infty}^x e^{-\frac{t^2}{2}} dt, \\ C_k &\triangleq \frac{(-1)^{k+1}}{k}, \\ B_k &\triangleq \frac{2(-1)^{k+1}}{k+1} \sum_{j=1}^k \frac{1}{j}, \\ G_1(\sigma, m) &\triangleq m\Phi\left(\frac{m}{\sigma}\right) + \frac{\sigma}{\sqrt{2\pi}} e^{-\frac{m^2}{2\sigma^2}} + \sum_{k=1}^{\infty} C_k [F(\sigma, m, k) + F(\sigma, -m, k)], \\ G_2(\sigma, m) &\triangleq (m^2 + \sigma^2) \Phi\left(\frac{m}{\sigma}\right) + (m + \log 4) \frac{\sigma}{\sqrt{2\pi}} e^{-\frac{m^2}{2\sigma^2}} \\ &\quad + 2 \sum_{k=1}^{\infty} C_k (m - k\sigma^2) F(\sigma, m, k) + \sum_{k=2}^{\infty} B_{k-1} [F(\sigma, m, k) + F(\sigma, -m, k)], \\ G_3(\sigma, m) &\triangleq \sigma^2 \sum_{k=0}^{\infty} (-1)^k [F(\sigma, m, k) + F(\sigma, m, k+1)]. \end{aligned}$$

**Example 1: Exponential Trigonometric Templates, Continued** Using the setting of Example 1, here we demonstrate an illustrative simulation to support the fundamental of our Poisson log-normal approximation: a sum of log-normal random vectors can be approximated by a log-normal random vector again.

When  $t = 1$ , a histogram of  $\log \Lambda(B_1, \eta)$  with  $B_1 = [0, 0.1]$  is shown in Figure 4, where 10,000 Monte Carlo GP paths  $\eta$  are drawn and we calculate

$$\Lambda(B_1, \eta) = \int_{B_1} e^{\eta(\nu)} d\nu.$$

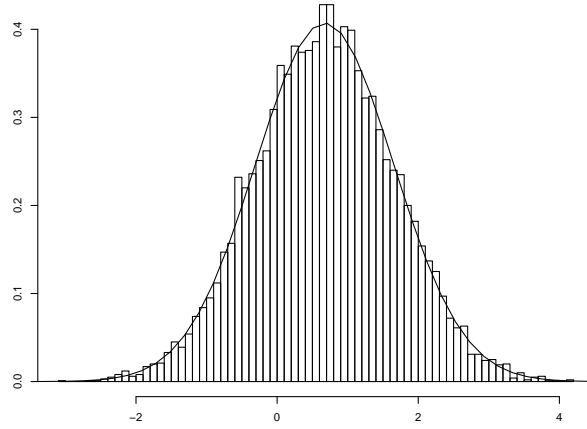


Figure 5: The histogram of  $\log \Lambda(B_1, \eta)$  for  $B_1 = [0, 0.1]$  as in Example 1 with 10,000 Monte Carlo samples. Also shown is the fitting of a normal distribution.

One can see that the normal distribution does quite a good job to approximate the distribution of  $\log \Lambda(B_1, \eta)$ , which means that  $\Lambda(B_1, \eta)$  can be approximated by a log-normal distribution. This is actually a general phenomenon, even valid for the multivariate case.

## C Sequential Monte Carlo Algorithm

---

**Algorithm 1** SMCS for BNS-ED

---

**Require:**

$N$ : the number of particles;  
 $M_U$ : the upper bound of observations;  
 $M_L$ : the lower bound of observations;  
 $c$ : the threshold of effective sample size (ESS);  
 $\epsilon$ : the threshold of information gain;  
Filters: the set of available filters and their bandwidths;  
 $\alpha$ : the prior parameter of the model weights;  
 $\tau$ : the step size of the Markovian move.

```
1: Draw  $\omega_0^{(i)} \overset{\text{i.i.d.}}{\sim} \text{Dir}(\alpha)$ ,  $i = 1, \dots, N$ .
2:  $\psi_0^{(i)} \leftarrow N^{-1}$ ,  $i = 1, \dots, N$ .
3: for  $t = 1, 2, 3, \dots$  do
4:   for  $i = 1, \dots, N$ ,  $y_t = M_L, \dots, M_U$ ,  $\nu_t \in \text{Filters}$  do
5:      $L_{t-1, y_t, \nu_t}^{(i)} \leftarrow p(y_t | \nu_t, \mathcal{F}_{t-1}, \omega_{t-1}^{(i)})$ .
6:   end for
7:   Calculate  $IG_t(\nu_t)$  with eq. (4),  $\nu_t \in \text{Filters}$ .
8:    $\nu_t \leftarrow \underset{\nu \in \text{Filters}}{\text{argmax}} IG_t(\nu)$ .
9:    $y_t \leftarrow \text{Observation at time } t$ .
10:   $\psi_t^{(i)} \leftarrow \psi_{t-1}^{(i)} \times L_{t-1, y_t, \nu_t}^{(i)}$ ,  $i = 1, \dots, N$ .
11:   $\psi_t^{(i)} \leftarrow \psi_t^{(i)} / \sum_{i'=1}^N \psi_t^{(i')}$ ,  $i = 1, \dots, N$ .
12:   $\omega_t^{(i)} \leftarrow \omega_{t-1}^{(i)}$ ,  $i = 1, \dots, N$ .
13:  if  $\text{ESS} \triangleq \left( \sum_{i=1}^N (\psi_t^{(i)})^2 \right)^{-1} < c$  then
14:    for  $i = 1, \dots, N$  do
15:      Draw  $\omega_{t,*}^{(i)} \overset{\text{i.i.d.}}{\sim} \sum_{i'=1}^N \psi_t^{(i')} \delta_{\omega_t^{(i')}}(\omega)$ .
16:       $\psi_t^{(i)} \leftarrow N^{-1}$ .
17:    end for
18:    // Markovian sampling.
19:    for  $i = 1, \dots, N$  do
20:      Draw  $\omega_{t,*}^{(i)} \sim \text{Dir}(\tau \omega_{t,*}^{(i)})$ .
21:       $A \leftarrow \text{Pr}(\omega_{t,*}^{(i)} \rightarrow \omega_{t,*}^{(i)})$ .
22:       $\omega_t^{(i)} \leftarrow \omega_{t,*}^{(i)}$  with probability  $A$ ,
23:       $\omega_t^{(i)} \leftarrow \omega_{t,*}^{(i)}$  otherwise.
24:    end for
25:  end if
26:   $L_{t, y_t, \nu_t}^{(i)} \leftarrow p(y_t | \nu_t, \mathcal{F}_{t-1}, \omega_t^{(i)})$ ,  $i = 1, \dots, N$ .
27:   $IG_t \leftarrow \sum_{i=1}^N \psi_t^{(i)} \log \left( \frac{L_{t, y_t, \nu_t}^{(i)}}{\sum_{i'=1}^N \psi_{t-1}^{(i')} L_{t-1, y_t, \nu_t}^{(i')}} \right)$ .
28:  if  $IG_t < \epsilon$  then
29:    Break.
30:  end if
31: end for
```

---